

# Combustion in thermonuclear supernova explosions

Friedrich K. Röpke

**Abstract** Type Ia supernovae are associated with thermonuclear explosions of white dwarf stars. Combustion processes convert material in nuclear reactions and release the energy required to explode the stars. At the same time, they produce the radioactive species that power radiation and give rise to the formation of the observables. Therefore, the physical mechanism of the combustion processes, as reviewed here, is the key to understand these astrophysical events.

Theory establishes two distinct modes of propagation for combustion fronts: subsonic deflagrations and supersonic detonations. Both are assumed to play an important role in thermonuclear supernovae. The physical nature and theoretical models of deflagrations and detonations are discussed together with numerical implementations. A particular challenge arises due to the wide range of spatial scales involved in these phenomena. Neither the combustion waves nor their interaction with fluid flow and instabilities can be directly resolved in simulations. Substantial modeling effort is required to consistently capture such effects and the corresponding techniques are discussed in detail. They form the basis of modern multidimensional hydrodynamical simulations of thermonuclear supernova explosions. The problem of deflagration-to-detonation transitions in thermonuclear supernova explosions is briefly mentioned.

---

Heidelberger Institut für Theoretische Studien, Schloss-Wolfsbrunnenweg 35, 69118 Heidelberg, Germany  
and  
Zentrum für Astronomie der Universität Heidelberg, Institut für Theoretische Astrophysik, Philosophenweg 12, 69120 Heidelberg, Germany  
e-mail: [friedrich.roepke@h-its.org](mailto:friedrich.roepke@h-its.org)

## 1 Introduction

Theory associates Type Ia supernovae with thermonuclear explosions of white dwarf stars. Therefore, any model of these spectacular astrophysical events is based on describing the physical processes leading to such explosions. Thermonuclear reactions release the energy necessary to overcome the gravitational binding of the star. What are these reactions? How do they spread over the stellar material after ignition? These questions are answered by combustion theory which was extensively developed for chemical terrestrial processes because of their importance for technical applications. Over the past two decades, there has been an increased interest in modeling the combustion processes in thermonuclear supernovae. As we will discuss below, the phenomena known from chemical combustion find many counterparts here. This led to a rapid improvement of multidimensional simulations of thermonuclear supernova explosions that greatly benefited from knowledge and techniques in technical combustion modeling. Some of the regimes of turbulent combustion that we will identify in the context of supernova modeling are encountered, for instance, in car engines, and are well known and studied there.

We will argue in the following sections that thermonuclear burning in Type Ia supernovae propagates as combustion waves subject to various instabilities. This makes the explosion physics of thermonuclear supernovae rich and its numerical simulation challenging. A variety of physical effects determine the propagation of such combustion waves, and the scales of interaction range from microscopic lengths below millimeters up to the radius of the exploding stars (thousands of kilometers). Modeling thermonuclear combustion in white dwarf stars is therefore a demanding multi-scale multi-physics problem.

## 2 Combustion in White Dwarf matter

The phenomenon of combustion is generally modeled as an interplay of fluid mechanics and reactions: reactions convert species and release the energy that drives the process. This causes fluid flow and energy transport that propagate the burning into fuel material. All this is captured in a set of partial differential equations that result from combining the Navier-Stokes equations of fluid dynamics with reactive and other source terms and additional terms that account for energy transport by diffusion and conduction. The equations are based on the concepts of mass conservation

$$\frac{\partial \rho}{\partial t} + \nabla \cdot (\rho \mathbf{v}) = 0, \quad (1)$$

momentum balance

$$\frac{\partial \rho \mathbf{v}}{\partial t} + \nabla \cdot (\rho \mathbf{v} \mathbf{v}) + \nabla \cdot \Pi = \rho \mathbf{f}, \quad (2)$$

species balance<sup>1</sup>

$$\frac{\partial \rho X_i}{\partial t} + \nabla \cdot (\rho X_i \mathbf{v}) = -\nabla \cdot (\rho \mathbf{v}_i^D X_i) + \rho \omega_{X_i} \quad i = 1 \dots N, \quad (3)$$

and energy balance

$$\frac{\partial \rho e_{\text{tot}}}{\partial t} + \nabla \cdot (\rho e_{\text{tot}} \mathbf{v}) + \nabla \cdot (\mathbf{v} \mathbf{\Pi}) = \rho \mathbf{v} \cdot \mathbf{f} + \rho \sum_{i=1}^N X_i \mathbf{v}_i^D \cdot \mathbf{f}_i - \nabla \cdot \mathbf{q} + \rho S. \quad (4)$$

Here,  $\rho$ ,  $\mathbf{v}$ ,  $e_{\text{tot}}$ ,  $\mathbf{\Pi}$ ,  $\mathbf{f}$ ,  $X_i$ ,  $\mathbf{v}^D$ ,  $\omega$ ,  $\mathbf{q}$ , and  $S$  denote mass density, fluid velocity, specific (i.e. per unit mass) total energy, pressure tensor, external forces, mass fraction of species  $i$  (index  $i$  running from 1 to the number of considered species  $N$ ), diffusion velocity, reaction rate, heat flux, and energy source terms due to reactions, respectively.

Eq. (1) equals the temporal change of the mass density to the divergence of the mass flux density (the sign is convention). Integrated over a control volume, Eq. (1) states that mass can only change inside it by a mass flux over its surface. Species, momentum, and energy are not strictly conserved. In addition to changes due to fluxes over the surface, they can be produced or destroyed by physical mechanisms inside the volume. This is captured in the source terms on the right-hand sides of Eqs. (3) – (4): momentum can be changed under the action of an external force, species are changed by diffusion and reactions, and energy is affected by external forces, diffusion processes, heat flux, and energy release or consumption in reactions. The list of source terms included in Eqs. (2) – (4) is not exhaustive. As pointed out by Timmes and Woosley (1992), radiative heat flux is unimportant in white dwarf matter, and we therefore neglect it here. The potential dynamic effects of magnetic fields are also not considered. Our choice of effects accounted for in the above equations, however, allows for a model that captures the basics of combustion physics in thermonuclear supernovae.

The system of Equations (1) – (4) is capable of describing complex physical processes. In particular, we emphasize the importance of the second term on the right-hand side of Eq. (2), the divergence of the momentum flux density, often referred to as “advection term.” This term is nonlinear in the fluid velocity leading to the rich (and theoretically still not satisfactorily understood) phenomenon of turbulence. Its impact on combustion processes will be discussed in Sect. 5. The ratio of the magnitude of the advection term to that of viscosity is measured by the Reynolds number  $Re$  on a certain spatial scale. In the situations encountered for thermonuclear burning in white dwarf stars, the value of the Reynolds number is huge (it can reach  $Re \sim 10^{14}$  on length scales comparable to that of the white dwarf star). To a good approximation, viscosity effects can be neglected in models that consider such astrophysical combustion processes on large scales. The pressure tensor then reduces to the hydrodynamical pressure  $P$ , and Eq. (2) simplifies to the Euler equation.

---

<sup>1</sup> Note that the combination of mass conservation with the equations describing balance of species overdetermines the system and thus Eqs. (1) and (3) have to be treated in a consistent way.

To close the system of Eqs. (1) – (4), an appropriate equation of state has to be provided. It relates pressure to other quantities such as mass density, internal energy, and composition. White dwarf stars are compact objects in which matter is fully ionized. For white dwarf matter, the ions dominate the mass density and are treated as an ideal gas. The electrons, however, provide the main contributions to pressure and energy. They form a degenerate gas and may be relativistic to a variable degree. Additional effects due to radiation, electron-positron pairs, and Coulomb interactions may also be incorporated in the equation of state. Unlike the ideal gas equation of state widely used in computational fluid dynamics, astrophysical equations of state are often provided in form of tables rather than as a closed expression. In addition, relations modeling heat flux and diffusion have to be specified. In the case of thermonuclear supernova explosions, the most important external force is gravity. The corresponding terms in the above equations can be determined from solving the Poisson equation for the given mass distribution.

Reaction rates and the energy source term due to reactions depend on temperature, density, and composition,

$$\begin{aligned}\omega_{X_i} &= \omega_{X_i}(\rho, T, X_i), \\ S &= S(\omega_{X_i}).\end{aligned}$$

The reactions in a combustion system can be chemical in nature, as is usually the case in terrestrial technical applications, or nuclear, as in Type Ia supernovae. Here, we are interested in the latter case. Nuclear reactions are formally treated with a nuclear reaction network (e.g. Hix and Meyer, 2006). This set of coupled ordinary differential equations describes the temporal change of the abundance of each species  $i$  due to electron captures,  $\beta$ -decays, photodisintegrations, two-, and three-body reactions (for higher-order reactions, the probability is low and they can be neglected). These effects depend on temperature, density, and the abundances of the other species in the system.

The numerical implementation of the hydrodynamics solver in thermonuclear supernova explosion simulations usually follows finite volume techniques. For a textbook on that matter we refer to Toro (2009).

Combustion is encountered in many situations in nature and technology. The characteristics of such processes, however, vary widely. Chemical combustion is classified depending on how the reactants are brought together in the fuel. In *premixed combustion*, all necessary ingredients for the reaction are contained in the fuel mixture, whereas diffusion processes bring the reactants into contact in *non-premixed combustion*. Both types are discussed in detail in Peters (2000). In thermonuclear supernovae, the fuel material contains all species required to set off nuclear burning, and therefore this situation resembles that of premixed combustion, which we will focus on in the following discussion.

### 3 Combustion fronts

Reactions in combustion systems are usually initiated by an ignition in a certain small volume from which they spread out. In the case of thermonuclear supernovae, the extremely strong dependence of the associated thermonuclear reaction rates on temperature localizes the burning in space so that it propagates as a combustion wave. For example, the reaction rate of carbon fusion, which initiates thermonuclear burning in carbon-oxygen white dwarf stars, scales at  $T \sim 10^{10}$  K as  $10^{12}$  (Hansen and Kawaler, 1994). Therefore, burning peaks sharply at the places of highest temperature, and the reaction is confined to a thin layer in space that propagates through the material. At high fuel densities, the width of such combustion waves may be tiny fractions of a millimeter. At lower densities it broadens, but it still remains small compared to the scales of the exploding white dwarf star with a radius of thousands of kilometers. The idealized treatment of a combustion wave as a sharp front, where fuel is instantaneously converted to ash and the corresponding energy is released, thus provides an excellent approximation for combustion modeling on these large scales.

This *discontinuity approximation* establishes the simplest model of a combustion wave. Its internal structure is not resolved, but the correct relation between the hydrodynamical states ahead and behind the combustion front is recovered. The discontinuity approximation simplifies the equations describing the system: microphysical transport due to diffusion and heat conduction can be neglected. If the fluid can be treated as ideal and in the absence of gravity and other external forces, the system reduces to the Euler equations with source terms due to reactions.

Discontinuities are not among the solutions of the system as stated above. This differential form of the equations of fluid dynamics allows only for continuous (“strong”) solutions. The integral form, however, also allows for discontinuous (“weak”) solutions. If treated in the differential form, discontinuous solutions require the introduction of additional jump conditions relating the hydrodynamical states on both sides of the discontinuity. Neglecting reactions, conservation of mass, momentum, and energy over discontinuities require continuous fluxes of these quantities over the discontinuity (which may carry jumps in other quantities such as density, temperature, etc.).

For simplicity, consider the system in one spatial dimension in the rest frame of the combustion front, and let  $u$  denote the velocity component normal to it. Combining the continuity of mass flux density,  $M := \rho u$ , and momentum flux density,  $\rho u^2 + P$ , over the front [the corresponding expressions can easily be read off from the terms on the left-hand side of Eqs. (1) and (2)], we arrive at the *Rayleigh criterion* (see Landau and Lifshitz, 1987) relating the unburnt and burnt states (denoted with subscripts “u” and “b”, respectively):

$$-M^2 = -(\rho_u u_u)^2 = -(\rho_b u_b)^2 = \frac{P_b - P_u}{V_b - V_u}. \quad (5)$$

The specific volume is defined as  $V := 1/\rho$ . Eq. (5) describes a straight line in the  $P$ - $V$ -plane. It must have a negative slope corresponding to  $-M^2$ , because the mass flux cannot be imaginary. The burnt state is characterized by a density and a pressure that is connected to the unburnt state by this line.

The Rayleigh criterion (5) derives from the principles of mass and momentum conservation and confines the *mechanically possible* burnt state to a line in the  $P$ - $V$ -plane. A second relation fixes the possible burnt states to a point. If no energy were released in the combustion wave, the energy flux  $(\rho e_{\text{tot}} + P)u = (1/2u^2 + e_{\text{int}} + P/\rho)\rho u$  over it would be continuous. Here, we introduce the specific internal energy  $e_{\text{int}} := e_{\text{tot}} - u^2/2$ . This results in a thermodynamic condition for the “burnt” state, the so-called *Hugoniot adiabat* (see Landau and Lifshitz, 1987):

$$e_{\text{int,u}} - e_{\text{int,b}} = -\frac{P_u - P_b}{2}(V_b - V_u). \quad (6)$$

Of course, no energy release in the burning is accounted for up to now, so it would be more correct to speak of the “post-discontinuity” state here; this is not done to avoid excessive introduction of notation. For common equations of state, the Hugoniot adiabat is a parabola in the  $P$ - $V$ -plane connecting the unburnt state to all *thermodynamically allowed* “burnt” states. It is important to note that the slope of the tangent to the Hugoniot adiabat at a certain point measures the speed of sound in the corresponding state, while the slope of the Rayleigh line through that same point represents the velocity of the front with respect to that state (see Landau and Lifshitz, 1987). The curve’s intersection with the Rayleigh line marks the *physically realized* (i.e. both mechanically and thermodynamically admissible) “burnt” state  $(V_b, P_b)$ .

The process modeled so far without energy release over the combustion front corresponds to a hydrodynamical shock. If energy release is considered, the Hugoniot curve shifts upward in the  $P$ - $V$ -plane and does not contain the unburnt state any longer:

$$e_{\text{int,u}} - e_{\text{int,b}} = \Delta h_0 - \frac{P_u - P_b}{2}(V_b - V_u). \quad (7)$$

Here,  $\Delta h_0$  denotes the difference in the formation enthalpies of the burnt and unburnt material. This situation is illustrated in Fig. 1. The shifted Hugoniot curve is usually referred to as *detonation adiabat*. It can intersect with Rayleigh lines issuing from the unburnt state  $(V_u, P_u)$  for different values of  $M$ . Since these lines must have a negative slope, the possible burnt state is located on one branch of the detonation adiabat, either above point  $A$  or below point  $A'$  in Fig. 1. Combustion in these two branches is caused by different physical mechanisms as we will discuss below.

The speed of sound in the unburnt material is graphical represented by slope of the tangent to the Hugoniot adiabat in point  $(V_u, P_u)$ . By construction (see Fig. 1), all Rayleigh lines connecting  $(V_u, P_u)$  to the upper branch of the upward-shifted detonation adiabat have a steeper slope, which, in turn, measures the velocity of the combustion wave with respect to the unburnt state Landau and Lifshitz (1987). This means that all processes leading to burnt states on the upper branch of the detonation adiabat are caused by combustion fronts that propagate supersonically with respect to the fuel. These are called *detonations*. The converse holds for burnt states

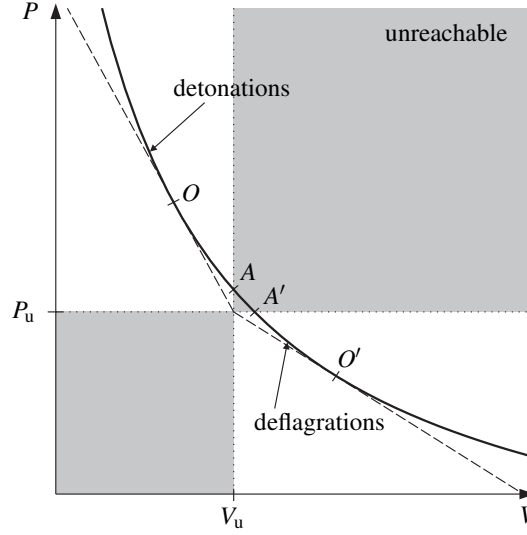


**Fig. 1** Relation between unburnt and burnt states in the discontinuity approximation of combustion. The detonation adiabat is plotted as a solid curve, and the tangential Rayleigh lines are dashed. [See also Landau and Lifshitz (1987) and Liñan and Williams (1993). Reprinted with minor modifications from Röpke (2003)]

on the lower branch of the detonation adiabat, and the corresponding subsonically propagating combustion fronts are called *deflagrations*.

The Rayleigh lines from  $(V_u, P_u)$  to the points  $O$  and  $O'$  in Fig. 1 mark a special case and are indicated with dashed lines in the figure. They are tangents to the detonation adiabat. With the same lines of arguments as above, one can show Landau and Lifshitz (1987) that combustion waves terminating in points  $O$  and  $O'$  propagate with the speed of sound in the burnt material. These are the so-called *Chapman-Jouguet* points. Above these points, the velocity of the front is subsonic with respect to the burnt state; below it is supersonic.

## 4 Deflagrations in White Dwarf matter

The simplified picture of a combustion front modeled as a discontinuity discussed in Sect. 3 provides useful relations between burnt and unburnt states that directly derive from the balance laws of fluid dynamics. It does not, however, address the question of the physical processes that lead to the phenomenon of propagating combustion waves on a microscopic level.

In contrast to detonations (see Sect. 7), deflagrations propagate due to micro-physical transport processes. Energy is released by reactions in the burning zone. Conduction and diffusion lead to a heating of the fuel ahead of this zone so that it

also reaches conditions for burning. In this sense, deflagrations resemble the picture of a propagating *flame front*. Its velocity is given by the microphysical transport processes and therefore slow compared to detonations that will be discussed below.

The full structure of deflagration waves results from solving Eqs. (1) – (4). The reaction zone, where the reaction rate is significant, typically occupies only a small fraction of the width of the structure, and it trails a more extended preheat zone.

Deflagrations in white dwarf matter are more complex than this schematic picture suggests. To solve the equation of combustion hydrodynamics, the relevant microphysical processes have to be modeled. Nuclear burning proceeds in a multitude of reactions, starting out with carbon burning, over oxygen burning to silicon burning, finally reaching nuclear statistical equilibrium, provided the fuel densities are sufficiently high. The relevant reactions have to be identified, and the corresponding reaction rates have to be provided. In addition, energy transport has to be accounted for. It turns out that the most important of these effects is thermal conduction, an energy flux caused by a temperature gradient:

$$\mathbf{q} = -\sigma \nabla T. \quad (8)$$

In white dwarf matter, different energy carriers are present, e.g., electrons, ions, and photons. The transport properties of these carriers have to be accounted for in determining the thermal conductivity  $\sigma$ . Timmes and Woosley (1992) discuss the corresponding contributions and conclude that electron conduction dominates over all other effects under conditions typical for white dwarf stars. The reason is that final states for electronic scattering processes are occupied below the difference of Fermi energy  $E_F$  of the electron gas, which is  $\sim 1$  MeV, and the thermal energy  $k_b T \sim 10$  keV. This implies extremely large mean free paths of the electrons leading to high values of  $\sigma$ .

An important consequence is observed when comparing the magnitudes of thermal conduction and diffusive energy transport, a ratio that defines the Lewis number. Typical values for white dwarf matter are  $\sim 10^7$  (Timmes and Woosley, 1992), while the Lewis number is order of unity in terrestrial combustion processes. The Prandtl number compares viscous transport to thermal conduction, and its value is typically very small in white dwarf matter (Timmes and Woosley, 1992). These figures of merit reflect the efficiency of electron conduction due to the high degeneracy of white dwarf matter. This situation greatly simplifies the solution of the equations of combustion hydrodynamics (1) – (4). The huge Lewis number indicates that diffusive processes are unimportant for the energy transport and can be neglected. The low value of the Prandtl number demonstrates the subdominance of viscous effects. Therefore, a model neglecting diffusive transport and based on the Euler equations of hydrodynamics rather than on the Navier-Stokes equations is justified. Another argument for this approach is that the full set of equations can only be solved numerically. Hydrodynamics solvers, however, introduce a considerable numerical viscosity, and explicitly accounting for small physical viscosities is pointless.

Numerical solutions of the resulting system determine the laminar (i.e. in case of a planar front in the absence of any geometrical perturbation) propagation speed  $s_1$



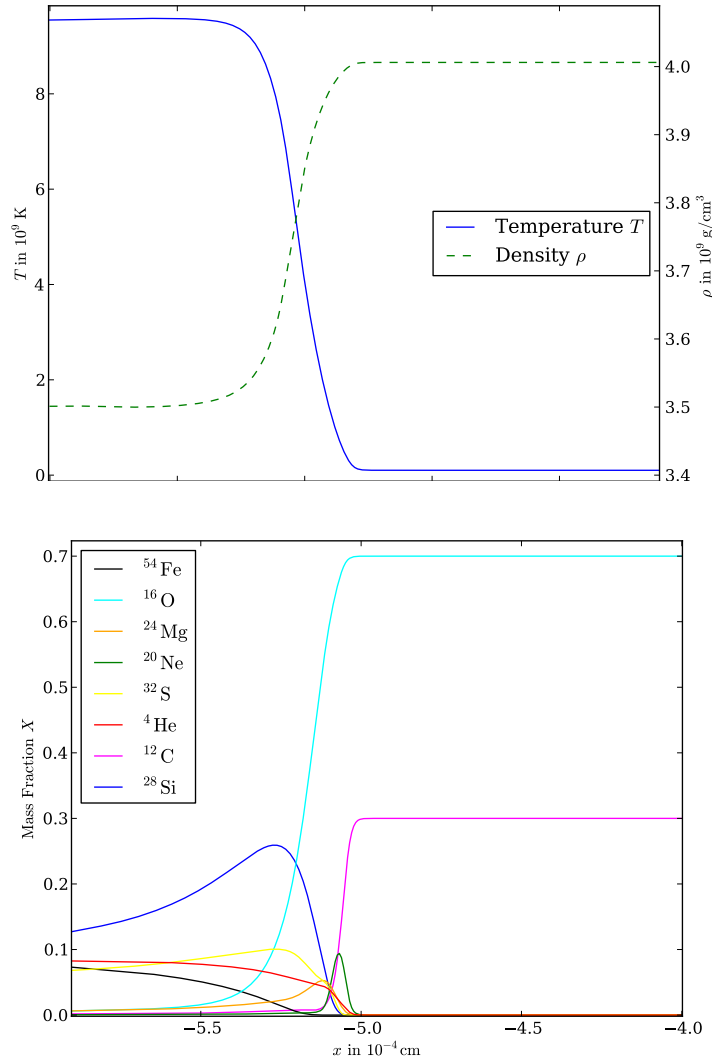


**Fig. 2** Structure of a deflagration flame for fuel at  $4 \times 10^9$  g cm<sup>-3</sup> with a composition of 30% carbon and 70% oxygen. Here, the flame advances from left to right. [Reprinted from the diploma thesis of Philipp Edelmann, Technische Universität München (2010), with permission of the author]

of deflagration waves as a function of fuel density, temperature, and composition. Results are given by Timmes and Woosley (1992). The different reactions occurring in a deflagration in white dwarf matter are illustrated in Fig. 2. It shows the density, the temperature, and the abundances of different species inside the structure. Note that the thermodynamical structure evolves monotonically, although the

various reactions give rise to burning on different length scales due to differences in their reaction rate. Therefore, the width of the “carbon flame” is almost an order of magnitude smaller than that of the “oxygen flame.”

## 5 Deflagration Instabilities and interaction with turbulence

In more than one spatial dimension, subsonic deflagrations are subject to various instabilities. Some of them are relevant or even fundamental for flame propagation in thermonuclear supernovae. Deflagrations in Chandrasekhar-mass white dwarfs are one prominent example. They can potentially unbind the stars (e.g. Reinecke et al., 2002b; Gamezo et al., 2003; Röpke et al., 2007a), or at least lead to the ejection of a substantial part of their masses (Jordan et al., 2012b; Kromer et al., 2013; Fink et al., 2014). This is not trivial as subsonic deflagrations significantly expand of the fuel material ahead of them due to their energy release. This drop in fuel density eventually inhibits further burning, and there is a competition between the star’s expansion and the fuel consumption by the flame. A simple laminar flame propagates too slowly. It does not burn sufficient amounts of material to explode the star. The required efficiency in energy release and species conversion is only possible due to the action of instabilities causing turbulence with which the flame interacts and thus accelerates. We will discuss below that instabilities are an inevitable physical consequence of any multidimensional treatment of fluid dynamics and flame propagation. These effects can only be parametrized in one-dimensional models, and thus a multidimensional simulations are mandatory when a solid and predictive explosion model is aimed for.

Not all potential flame instabilities are relevant for the case of thermonuclear burning in supernovae. The diffusive-thermal instability (Barenblatt et al., 1962), for instance, is suppressed at the prevailing high Lewis numbers. The three main instabilities that potentially affect the flame propagation are the Rayleigh-Taylor instability, the Kelvin-Helmholtz instability, and the Landau-Darrieus instability. The first two are general fluid flow instabilities, while the latter is specific to burning fronts.

The Rayleigh-Taylor instability is caused by buoyancy in the corresponding supernova explosion scenarios. The flame ignites near the stellar center and burns toward the surface. Behind the flame, energy is released by nuclear reactions. This partially lifts the degeneracy, and therefore the density in the ashes is lower than in the fuel. The result is an inverse density stratification in the gravitational field of the star, which is buoyancy unstable. Perturbations at the interface between fuel and ash grow. In the nonlinear stage, the Rayleigh-Taylor instability leads to the formation of bubbles of hot ash material that rise into the cold fuel. In between, downdrafts transport fuel material toward the star’s center. These counterflows at the fuel-ash interface lead to shear at the flame. The Kelvin-Helmholtz instability amplifies initial perturbations and forms a wave pattern that grows into eddies in the nonlinear stage.

The flame itself, however, is subject to an instability that arises from its self-propagation. This so-called Landau-Darrieus instability is active on all scales that are significantly larger than the internal flame width and results from a refraction of stream lines in the vicinity of a flame front due to the change in density over it. While the tangential velocity component over the front is steady, mass flux conservation requires a jump in the normal component. This widens streamlines in the vicinity of bulges of the flame and consequently the fluid velocity is lower locally. The laminar burning speed is thus larger than the local fluid velocity and this causes bulges to increase. Recesses become deeper by the opposite effect. Thus perturbations deforming the flame front from planar geometry grow.

In the nonlinear regime, however, the flame stabilizes into a cellular pattern (Zel'dovich, 1966). Such a stabilization was shown to be effective for thermonuclear flames in white dwarf matter (Röpke et al., 2003, 2004a,b). The Landau-Darrieus instability is therefore not expected to have a significant impact on burning in thermonuclear supernovae.

The Rayleigh-Taylor and Kelvin-Helmholtz instabilities, in contrast, show no such nonlinear stabilization. They are fundamental for the evolution of flame structure on the scales of the exploding white dwarf star and lead to a considerable acceleration of burning in thermonuclear supernovae. Both instabilities, however, do not act on the smallest spatial scales. The growth time of the Rayleigh-Taylor instability competes with the burning time scale. At the smallest scales front distortions grow so slowly that they will be overrun by the flame. As the growth time of the buoyancy-driven instability increases with the length scale of the perturbations, there exists a minimum scale for the Rayleigh-Taylor instability develop in the presence of a self-propagating flame. This so-called fire-polishing length can be estimated as (see also Timmes and Woosley, 1992)

$$\lambda_{\text{fp}} = \frac{g s_{\text{f}}^2}{2\pi} \frac{\rho_{\text{u}} - \rho_{\text{b}}}{\rho_{\text{u}} + \rho_{\text{b}}}, \quad (9)$$

with  $g$  denoting the gravitational acceleration.

The Kelvin-Helmholtz instability acts as a secondary effect, because the shear motions necessary to trigger it are produced by the large-scale uprising plumes of hot ashes in the nonlinear stage of Rayleigh-Taylor instability. In its nonlinear regime, the Kelvin-Helmholtz instability results in vortices that develop in the shear region. A prerequisite for a Kelvin-Helmholtz unstable configuration is a tangential discontinuity without a flow over it. This is clearly not the case encountered for burning fronts. The finite mass flow over them stabilizes flames against the Kelvin-Helmholtz instability. Its effect is similar to that of viscosity in shear layers leading to some stabilization. With buoyancy acting to form fast-rising bubbles of ash, however, the situation changes. The resulting shear velocities are much larger than the flow velocities over the flame fronts. Indeed, in numerical simulations Niemeyer and Hillebrandt (1997) found that the flame becomes subject to the Kelvin-Helmholtz instability once the shear velocity exceeds the laminar burn-

ing speed. This is typically the case for thermonuclear deflagrations in white dwarf stars.

The action of the Kelvin-Helmholtz instability is the primary cause for the generation of turbulence. The importance of this effect can be estimated from the Reynolds numbers of the shear flows around rising bubbles of burning material that are as high as  $10^{14}$ . This gives rise to the following picture: turbulent eddies are generated by shear instability at the location of the flame at the large scales of the buoyant plumes of burnt material. These eddies themselves are unstable and decay to smaller eddies, thus establishing a turbulent cascade. In this cascade, turbulent kinetic energy injected at the largest scales is transported without loss through the so-called inertial range. The velocity of the turbulent eddies steadily decreases toward smaller scales. At some microscopic scale (much below a millimeter), the local (scale-dependent) Reynolds number drops to  $\sim 1$  indicating that viscous effects become important. At this so-called Kolmogorov scale they dissipate the turbulent kinetic energy into heat.

The flame interacts with turbulent eddies on a wide range of scales. On scales much larger than its internal width, they deform and corrugate the flame front. The scale down to which this effect is active depends on the flame speed. Similar to the argument of the fire polishing length for buoyancy instability, there should be a scale on which the turbulent eddy velocities have become so low that they are comparable to the laminar flame speed. This implies that below this so-called *Gibson scale*  $l_{\text{Gib}}$  the flame burns faster through the turbulent eddies than they turn over, and the flame is nearly undistorted by the action of eddies. For constant turbulent velocities, the size of the Gibson scale depends on the fuel density. With lower fuel density the flame speed decreases and the Gibson scale becomes smaller (see Fig. 3).

One important question is how far down in scale space the effect of turbulent velocity fluctuations affects the flame, i.e. the size of the Gibson scale. If this scale is significantly above the width of the flame, turbulence will not interact with the internal flame structure. The only effect is then a corrugation of the flame front on large scales. This is the so-called *flamelet regime* of turbulent combustion (Peters, 2000). While the microphysics of the burning is unaffected and the laminar flame speed does not change, the overall flame wrinkling has significant effect on the overall burning efficiency. The flame surface is enlarged and therefore the net burning rate increases.

If, however, the Gibson scale is smaller than the internal flame width, turbulent eddies will affect the internal flame structure. They can now transport material into and out of the flame structure and thus disrupt it. This is the so-called *distributed burning regime*. Depending on the size of the Gibson scale, different sub-regimes are distinguished (see Peters, 2000, for an extensive discussion): In the *thin reaction zone regime*, turbulence will alter the structure of the preheat zone, but not the reaction zone itself. When the Gibson scale reaches down to the width of the actual reaction zone, burning is said to take place in the *broken reaction zones regime* and ultimately turbulence completely dominates the burning process and spreads it out over space in the *well-stirred reactor regime*.

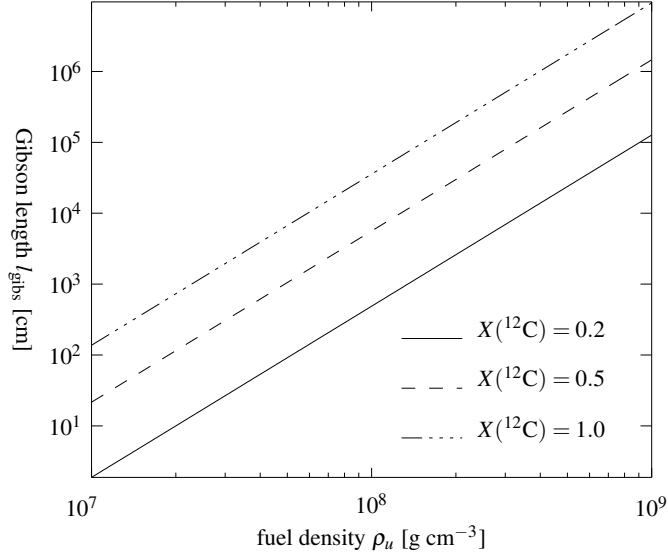


**Fig. 3** Gibson scale for typical deflagrations in Chandrasekhar-mass white dwarf stars as a function of fuel density for different carbon mass fractions in the white dwarf material. [Reprinted from Röpke (2003)]

In a thermonuclear supernova explosion resulting from a deflagration, the flame will enter the distributed burning regime. Towards the end of the burning, turbulence freezes out and the gravitationally unbound material approaches homologous expansion (Röpke (2005)). Before this happens, however, the flame will transition from the flamelet regime of turbulent combustion to the distributed burning regime. As the exploding white dwarf expands and the flame burns towards its surface, the fuel density decreases thus reducing the Gibson scale (see Fig. 3). At the same time, the internal width of the deflagration grows with decreasing fuel density (e.g. Timmes and Woosley, 1992). Once the flame reaches material with  $\lesssim 10^7 \text{ g cm}^{-3}$ , the Gibson scale falls below the flame width, and turbulence affects its internal structure.

Overall, the picture is that deflagrations in thermonuclear supernova explosions are far from propagating laminar. They possess a pronounced multidimensional structure, being wrinkled by instabilities on large scales, and the thus induced turbulence interacts with them on a wide range of scales. A one-dimensional model therefore is necessarily approximate and introduces free parameters. For a consistent treatment, multidimensional hydrodynamical simulations are inevitable.

## 6 Modeling deflagrations

The internal structure of deflagrations in the dense core of carbon-oxygen white dwarfs cannot be resolved in current multidimensional explosion simulations. Therefore, modeling approaches are required. Two general strategies can be distinguished that have been used in such simulations: The first broadens the flame artificially by tuning the microphysical transport coefficients and the progress of the reaction such that a structure emerges that can be resolved on the scale of the computational grid. The second approach treats the flame as a sharp discontinuity with no attempt to model its internal structure. It has to be emphasized that neither of the approaches captures the physical processes inside the flame correctly.

The approach of artificially broadened flames was introduced to the field of thermonuclear supernova simulations by Khokhlov (1995) (see also Vladimirova et al., 2006; Calder et al., 2007). It is based on a reaction progress variable  $\phi$  that governs energy release and species conversion. The evolution of  $\phi$  is described by an advection-diffusion-reaction (ADR) equation

$$\frac{\partial \phi}{\partial t} + \mathbf{v} \cdot \nabla \phi = \kappa \nabla^2 \phi + \frac{1}{\tau} R(\phi), \quad (10)$$

and hence the flame model is often referred to as ADR approach. In the absence of advection ( $\mathbf{v} = 0$ ),  $\phi$  is propagated by diffusion and produced by reaction. The diffusion coefficient  $\kappa$  and the time scale of the reaction  $\tau$  do not reflect microphysical processes but are model parameters chosen such that the global flame properties are obtained in the desired way: a model flame is defined that matches the laminar flame propagation speed of the physical flame but is broad enough to be resolved with a few cells on the computational grid. A more sophisticated version of this flame model involves individual progress variables for the different burning stages in the flame (carbon consumption, oxygen consumption and burning of silicon group elements to nuclear statistical equilibrium, see Calder et al., 2007).

The level-set approach, in contrast, models the flame as a discontinuity. Energy is released, and species are converted instantaneously at the position of the discontinuity. Such a discontinuity can be treated numerically by associating it to the zero-level set of a signed distance function  $G(\mathbf{x}, t)$ ,  $|\nabla G| = 1$ , such that the flame is modeled as the moving hypersurface  $\Gamma(t)$ :

$$\Gamma(t) := \{\mathbf{x} | G(\mathbf{x}, t) = 0\} \quad (11)$$

(Osher and Sethian, 1988). The propagation of this hypersurface is given by the evolution of the signed distance function

$$\frac{\partial G}{\partial t} = (\mathbf{v}_u \mathbf{n} + s_u) |\nabla G|, \quad (12)$$

where  $\mathbf{v}_u$ ,  $\mathbf{n}$ , and  $s_u$  denote the fluid velocity in the unburnt material, the normal vector to the flame front, and the flame speed with respect to the fuel, respectively.

The  $G$ -function is defined to be negative in the fuel and positive in the ashes (for details of the implementation of the level-set approach for thermonuclear flames in white dwarf material see Reinecke et al., 1999). From  $G$ , the location of the flame can be reconstructed with subgrid cell resolution.

Clearly, both approaches do not consistently treat the burning microphysics but are models to propagate a flame-like structure on scales resolvable in a thermonuclear supernova simulation. Therefore, the model parameters have to be calibrated to reproduce properties of the physical flames (in particular the flame speed and the energy release). These have to be known independently and are taken from one-dimensional microscopic flame simulations (e.g. Timmes and Woosley, 1992). Both the ADR and the level-set approaches are widely used to model deflagrations in thermonuclear supernova explosion simulations. Although the ADR model may seem physically better motivated, it has disadvantages: because the model flame has an artificial finite width, it suffers from curvature effects close to the grid scale, and it modifies fluid flows in neighboring cells that are physically very far away from the actual flame. This may alter the response of ADR model flames to instabilities and turbulence. Minimizing such effects is one of the reasons why ADR approaches are usually combined with adaptive mesh refinement (AMR) techniques. The level-set approach, in contrast, is in principle able to localize the flame front with subgrid-scale resolution as a discontinuity (in the hydrodynamical variables, at least as much as the employed hydrodynamics solver is able to represent discontinuities), and AMR is usually not employed here.

As discussed in Sect. 5, flames do not propagate laminar in white dwarfs. They are subject to instabilities and interaction with turbulent motions, which significantly enhances the burning efficiency. Such effects have to be taken into account in any flame model for simulating thermonuclear supernova explosions. This is not automatically guaranteed because of the finite spatial resolutions these simulations reach. Consequently, the numerical flame model will lack structure from the unresolved scales and be artificially smooth. For the flamelet regime, surface area enhancement and burning acceleration due to flame-turbulence interaction are therefore not fully reproduced in simulations. To compensate for the effect of missing flame substructure, the model flame front is propagated on the grid scale with an effective *turbulent flame speed*  $s_t$  instead of the laminar value  $s_l$ , that applies only to unresolved microscopic scales. This is critical for the success of many thermonuclear supernova models.

An approach used in some of the published thermonuclear supernova simulations (e.g. Gamezo et al., 2003; Jordan et al., 2008; Townsley et al., 2007; Jordan et al., 2012b) is to scale the effective turbulent flame speed to the velocity of buoyantly rising bubbles

$$s_t \propto \sqrt{gL \frac{\rho_u - \rho_b}{\rho_u + \rho_b}}, \quad (13)$$

where  $g$  is the gravitational acceleration and  $L$  denotes the length scale of the bubble, here associated to the scale of the computational grid. Khokhlov (1995) discusses a self-similarity in structures of turbulent flame fronts subject to buoyancy as a motivation for this approach.

The assumption of turbulent flame speeds being set by buoyancy effects has been called into question by Ciaraldi-Schoolmann et al. (2009), who argue that a turbulence-driven speed should be used instead (but see Hicks, 2015). An elaborate technique to account for flame-turbulence interaction is based on turbulent subgrid-scale models. According to Damköhler (1940) the turbulent burning speed  $s_t$  of a flame on a certain scale should be proportional to the turbulent velocity fluctuations  $v'$  on that scale. These are determined from a subgrid-scale turbulence model in a Large-Eddy Simulation (LES) approach. In an LES, only the largest scales of the turbulent cascade, where energy is injected into it, are resolved together with the onset of the inertial range. At the grid scale, the turbulent energy cascade is cut off, and additional modeling is required at and below this scale. Such turbulent subgrid-scale models were introduced by Niemeyer and Hillebrandt (1995), Schmidt et al. (2006a,b) to the field of thermonuclear supernova explosion simulations (see Jackson et al., 2014, for an alternative approach). They are based on a balance equation that describes the budget of turbulent kinetic energy on the unresolved scales, with terms accounting for transport of kinetic energy from the resolved to the unresolved scales, for energy transport on the unresolved scales, for dissipation by viscosity on unresolved scales, and for the action of the Archimedian force on unresolved scales. These subgrid-scale models for turbulence-flame interactions were used in several multidimensional simulations of deflagrations in white dwarfs leading to thermonuclear supernova explosions, e.g., Reinecke et al. (2002a,b), Röpke and Hillebrandt (2004, 2005), Röpke (2005), Röpke et al. (2006, 2007a,b), and Fink et al. (2014).

## 7 Detonations

The physical mechanism of detonations differs fundamentally from that of deflagrations. A detonation propagates due to the progression of a shock wave that compresses and heats fuel material such that it starts to burn. This burning, in turn, releases the energy to further support the shock wave. The temperature increase enhances the reaction rate – a process, however, that proceeds more slowly because the shock structure is too thin to allow significant reactions while passing. Behind this shock wave, reactions take place and release energy leading to a further increase in temperature which also raises the reaction rate. Fuel is consumed until depleted. Unlike deflagrations, the propagation of detonations is not determined by microphysical transport processes, but instead by hydrodynamical effects. Consequently, these are fast combustion fronts advancing with the speed of the shock wave supersonically with respect to the fuel state.

For planar detonations, a theoretical picture was independently developed by Zel'dovich (1940), von Neumann (1942), and Döring (1943). This so-called ZND model can be illustrated in the  $(P, V)$ -plane of Fig. 1. Consider the detonation branch only (see Fig. 4). The shock in the ZND model is assumed to be infinitely thin as in the discontinuity approximation discussed in Sect. 3. It evolves the initial state



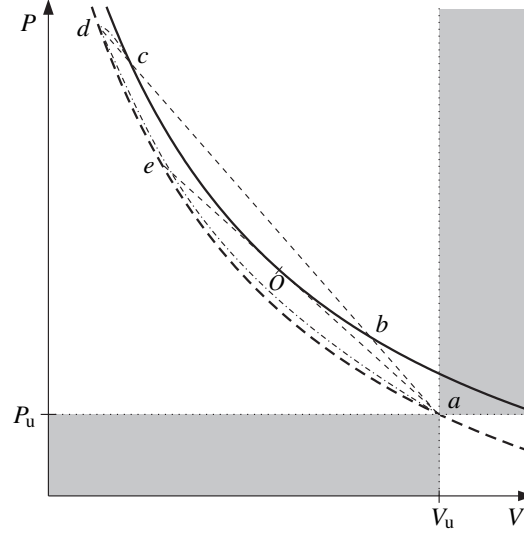


**Fig. 4** Close-up of the detonation branch. [See also Landau and Lifshitz (1987) and Liñan and Williams (1993). Reprinted with minor modifications from Röpke (2003)]

from point  $a$  along the detonation adiabat (bold dashed curve) over point  $e$  to state  $d$ , which marks the highest pressure in the detonation structure and is called the *von Neumann spike*. Here, reactions set in and lead to a heating and expansion of the material. Contrary to the above-discussed discontinuity approximation, the reactions are no longer assumed to be instantaneous but proceed with finite rates behind the shock. The corresponding path toward the final burnt state, e.g.  $c$ , must follow down a Rayleigh line, i.e.  $dc$ , because mass and momentum are conserved for all intermediate states. This path can be pictured as consisting of a sequence of intermediate states in which adiabats corresponding to partial but progressively more complete burning intersect with the Rayleigh line until the detonation adiabat of the full energy release is reached. Relaxing the assumptions of the ZND theory leads to a more realistic path that is indicated as a dashed-dotted line in Fig. 4.

A special case is obtained when the final state is located at the Chapman-Jouguet point  $O$ . The detonation then propagates sonically with respect to the burnt material. Detonations often propagate in this mode and attain a steady structure (see Fickett and Davis, 1979, for a more comprehensive treatment of detonation theory). In white dwarf material of sufficiently high density to burn to nuclear statistical equilibrium, detonations diverge from the Chapman-Jouguet type because of the endothermic nature of the involved photodissociation reactions (Khokhlov, 1989; Sharpe, 1999; Gamezo et al., 1999). They are of pathological type and travel with greater speeds. At lower densities, however, the Chapman-Jouguet case is a valid approximation.

## 8 Multidimensional structure of detonations

The detonation model outlined above describes the simplified one-dimensional case of planar detonation waves. Because detonations propagate into the fuel with supersonic speeds, they are not subject to external hydrodynamical instabilities, such as the Rayleigh-Taylor or the Kelvin-Helmholtz instabilities. Nonetheless, real detonations possess a three-dimensional structure. Planar detonations are unstable and form incident shocks, transverse shock waves, and triple points. Their continuous interactions cause the emergence of cellular patterns (e.g. Fickett and Davis, 1979) that are observed in terrestrial experiments.

Transverse waves move back and forth along the detonation perpendicular to its direction of motion. At the points where they collide, so-called triple points emerge. Between these triple points, the shocks show significant curvature and are too weak to sustain the detonation. In the triple points, the compression is stronger, and this drives the reactions and the propagation of the detonation. The tracks of these triple points form a cellular pattern in the downstream material. This effect is observed in small-scale simulations of thermonuclear detonations in white dwarf matter (Boisseau et al., 1996; Gamezo et al., 1999; Timmes et al., 2000). It alters the characteristics of the detonation. Burning is more complete in the triple points, and thus the chemical composition of the ashes is inhomogeneous behind the front with pockets of less completely burned material off the paths of the triple points. The emerging complex multidimensional detonation structure is widened compared to the prediction of the one-dimensional model, and its propagation speed is lower.

The one-dimensional theory therefore applies only in an average sense and provides an acceptable approximation if multidimensional structure cannot be resolved. According to Gamezo et al. (1999), this is the case for detonations in dense white dwarf material. At lower densities, these structures may grow to sizes comparable to the scales of the exploding star. Even if unresolved, the changes in propagation velocity and ash composition due to the multidimensional structure may affect the characteristics of thermonuclear supernova explosions, although not by much (Timmes et al., 2000). Overall, multidimensional detonations are weaker and may quench at higher densities than expected from one-dimensional theory.

## 9 Modeling detonations

In many models of thermonuclear supernova explosions, detonations play an important role. They seem to be required to produce the stratified chemical composition observed in the outer layers of normal Type Ia supernovae. Because the associated shock wave compresses the material, they lead to more complete burning than deflagrations for the same fuel density. To produce the intermediate mass elements observed in the spectra of Type Ia supernovae, substantial burning has to take place in low-density material. This is not given for detonations in Chandrasekhar-mass white dwarfs in hydrostatic equilibrium. The high densities in these would lead to

an exclusive production of iron group elements. Therefore, detonations have to trigger after a phase of expansion caused by an initial deflagration in a Chandrasekhar-mass white dwarf, or they lead to explosions of less compact sub-Chandrasekhar mass configurations.

Contrary to the case of deflagrations, detonations do not rely on microphysical transport, but arise directly from reactive fluid dynamics. Therefore, no additional modeling of microphysical processes is required for capturing these processes in numerical simulations that are based on the reactive Euler equations. In multidimensional simulations of thermonuclear explosions of white dwarfs, however, it is impossible to resolve the inner structure of detonations. Similar to the case of deflagrations, two approaches have been taken: one that broadens the structure to fit on the numerical grid and one that treats detonations as sharp discontinuities.

Broadened detonations arise naturally in a system modeled with the reactive Euler equations, provided they are triggered and the thermodynamic conditions are sufficient to allow for their propagation. The correct jumps in the hydrodynamical quantities as well as the detonation speed are retained for Chapman-Jouguet detonations even if their microphysical structure is not resolved. This means that contrary to broadened deflagrations, the detonation speed is determined consistently in the model and does not have to be provided externally. It is, however, necessary to artificially suppress unphysical burning inside the (too wide) shock structure. This approach has been employed in a number of thermonuclear supernova simulations (Gamezo et al., 2005; Meakin et al., 2009; Townsley et al., 2009; Jackson et al., 2010; Jordan et al., 2012a; Moll and Woosley, 2013; Pakmor et al., 2013, e.g.).

The level-set approach allows to numerically treat detonations as discontinuities and has been employed in simulations of thermonuclear supernovae (e.g. Golombek and Niemeyer, 2005; Röpke and Niemeyer, 2007; Kasen et al., 2009; Sim et al., 2010; Fink et al., 2010; Pakmor et al., 2010, 2012; Seitenzahl et al., 2013; Ohlmann et al., 2014; Marquardt et al., 2015; Seitenzahl et al., 2016). Here, the material crossed by the model detonation is instantaneously converted into nuclear ash, and the corresponding energy is released. This does not require to include an extensive reaction network as the details of the burning are not resolved. Therefore, energy release, species conversion, and detonation speed are parameters of the model that have to be determined externally. Such a parametrization can lead to inaccuracies, and, therefore, contrary to the case of deflagrations, it may be preferred to use the broadened detonations approach. The advantages of the level-set technique, however, are that unphysical propagation of detonations over deflagration ash regions (Maier and Niemeyer, 2006) in the delayed detonation model can easily be prevented and that the speed of non-Chapman-Jouguet detonations can be correctly set.

## 10 Deflagration-to-detonation transitions

The model of delayed detonations for Type Ia supernova explosions (Khokhlov, 1991) assumes a spontaneous transition of the burning mode from an initial subsonic deflagration to a supersonic detonation. Such transitions are indeed observed in terrestrial combustion, where they are usually arise from the interaction of the deflagration flame with walls or obstacles in the combustion region. In the case of thermonuclear supernovae, deflagration-to-detonation transitions (DDTs) have to take place in an unconfined medium. It is unclear, however, whether such unconfined DDTs occur in nature.

One possibility (but see Poludnenko et al., 2011, for an alternative) is a suitable spatial gradient of autoignition delay (also called *induction*) times of the reactions. Such a configuration may lead to a coherent runaway of the reactions with a phase velocity that is sufficient to ramp up to a detonation wave. The original idea of Zel'dovich et al. (1970) was later extended to the so-called shock wave amplification through coherent energy release (SWACER) picture by Lee et al. (1978).

This detonation initiation mechanism requires a preconditioning of the fuel material with a shallow temperature gradient to arrange for the required induction time gradient. It has been speculated that sufficiently strong turbulence in a late phase of deflagration burning in a thermonuclear supernova explosion can provide such conditions, in particular once the fuel density has dropped to  $\lesssim 10^7 \text{ g cm}^{-3}$  (Lisewski et al., 2000; Woosley et al., 2009), but it is difficult to identify such regions in simulations of thermonuclear supernova explosions (see Röpke, 2007, for a possibility). Several simulations therefore artificially prescribe the DDT spot or trigger the transition once the deflagration flame reaches a certain density threshold. Ciaraldi-Schoolmann et al. (2013) propose a subgrid-scale model for DDTs that takes into account turbulence properties. This model was employed in the delayed detonation simulations of Seitenzahl et al. (2013).

## 11 Conclusions

The theory of combustion provides the basis for models of thermonuclear supernova explosions. Because of its technological application, combustion is well studied, and theory of the basic phenomena has reached a rather mature state. It can therefore be claimed that the physical principles of combustion wave propagation – at least for the one-dimensional case – are understood to the level of precision needed for modeling the astrophysical events. Complications arise in multidimensional models because of instabilities and interaction with turbulence.

The numerical implementation of combustion waves remains challenging because of the limited spatial resolution in multidimensional supernova explosion simulations. Both deflagration and detonation propagation modes can either be represented as an artificially broadened structure fitting on the numerical grid or as a sharp discontinuity between fuel and ash. Advantages and disadvantages of both

approaches have been discussed. It seems that for deflagration modeling a discontinuity representation is favorable, while detonations are better captured in the broadened wave approach, but this may depend on the particular situation and explosion scenario under consideration. Different possibilities exist for modeling the interaction of deflagrations with instabilities and turbulence, and elaborate subgrid-scale techniques have been employed in supernova simulations. The multidimensional structure of detonations is not recovered (nor accounted for) in current thermonuclear supernova explosion simulations. Although it seems unlikely to have a significant impact on the results of such simulations in terms of ejecta composition and predicted observables, future model improvement may require to account for this effect.

Deflagration-to-detonation transitions in unconfined media are an unsolved problem in combustion theory. In delayed detonation models of Type Ia supernovae, this adds an uncertainty. Although necessary conditions for such a transition have been derived, it remains unclear whether the mechanism is actually realized in nature.

Current combustion wave models are successful in providing a qualitative picture of Type Ia supernova explosion scenarios. Future efforts, however, are required to make them precise enough to allow for a detailed quantitative comparison with observed supernova events.

**Acknowledgements** This research was supported by the Munich Institute for Astro- and Particle Physics (MIAPP) of the DFG cluster of excellence “Origin and Structure of the Universe.” In particular, participation in the MIAPP workshop “The physics of supernovae,” where this article was initiated, is gratefully acknowledged. The work of FKR is supported by the Klaus-Tschira Foundation.

## References

- Barenblatt, G. I., Y. B. Zel’dovich, and A. G. Istratov. 1962. On the diffusional-thermal stability of a laminar flame. *Zh. Prikl. Mekh. Tekh. Fiz.* 4: 21–26.
- Boisseau, J. R., J. C. Wheeler, E. S. Oran, and A. M. Khokhlov. 1996. The Multidimensional Structure of Detonations in Type IA Supernovae. *ApJ Lett.* 471: 99–102.
- Calder, A. C., D. M. Townsley, I. R. Seitenzahl, F. Peng, O. E. B. Messer, N. Vladimirova, E. F. Brown, J. W. Truran, and D. Q. Lamb. 2007. Capturing the Fire: Flame Energetics and Neutronization for Type Ia Supernova Simulations. *ApJ* 656: 313–332.
- Ciaraldi-Schoolmann, F., I. R. Seitenzahl, and F. K. Röpke. 2013. A subgrid-scale model for deflagration-to-detonation transitions in Type Ia supernova explosion simulations. Numerical implementation. *A&A* 559: 117.
- Ciaraldi-Schoolmann, F., W. Schmidt, J. C. Niemeyer, F. K. Röpke, and W. Hillebrandt. 2009. Turbulence in a three-dimensional deflagration model for Type Ia supernovae. I. Scaling properties. *ApJ* 696: 1491–1497.
- Damköhler, G. 1940. Der Einfluß der Turbulenz auf die Flammengeschwindigkeit in Gasgemischen. *Z. f. Elektroch.* 46 (11): 601–652.
- Döring, W. 1943. Über den Detonationsvorgang in Gasen. *Annalen der Physik* 435: 421–436.
- Fickett, W., and C. Davis. 1979. *Detonation. Los Alamos series in basic and applied sciences.* University of California Press.

- Fink, M., F. K. Röpke, W. Hillebrandt, I. R. Seitenzahl, S. A. Sim, and M. Kromer. 2010. Double-detonation sub-Chandrasekhar supernovae: can minimum helium shell masses detonate the core? *A&A* 514: 53.
- Fink, M., M. Kromer, I. R. Seitenzahl, F. Ciaraldi-Schoolmann, F. K. Röpke, S. A. Sim, R. Pakmor, A. J. Ruiter, and W. Hillebrandt. 2014. Three-dimensional pure deflagration models with nucleosynthesis and synthetic observables for Type Ia supernovae. *Mon. Not. R. Astron. Soc.* 438: 1762–1783.
- Gamezo, V. N., A. M. Khokhlov, and E. S. Oran. 2005. Three-dimensional delayed-detonation model of Type Ia supernovae. *ApJ* 623: 337–346.
- Gamezo, V. N., J. C. Wheeler, A. M. Khokhlov, and E. S. Oran. 1999. Multilevel Structure of Cellular Detonations in Type IA Supernovae. *ApJ* 512: 827–842.
- Gamezo, V. N., A. M. Khokhlov, E. S. Oran, A. Y. Chtchelkanova, and R. O. Rosenberg. 2003. Thermonuclear supernovae: Simulations of the deflagration stage and their implications. *Science* 299: 77–81.
- Golombek, I., and J. C. Niemeyer. 2005. A model for multidimensional delayed detonations in SN Ia explosions. *A&A* 438: 611–616.
- Hansen, Carl J., and Steven D. Kawaler. 1994. *Stellar interiors: physical principles, structure, and evolution. Astronomy and astrophysics library*. New York: Springer.
- Hicks, E. P. 2015. Rayleigh-Taylor unstable flames – Fast or faster? *ApJ* 803: 72.
- Hix, W. R., and B. S. Meyer. 2006. Thermonuclear kinetics in astrophysics. *Nuclear Physics A* 777: 188–207.
- Jackson, A. P., D. M. Townsley, and A. C. Calder. 2014. Power-law wrinkling turbulence-flame interaction model for astrophysical flames. *ApJ* 784: 174.
- Jackson, A. P., A. C. Calder, D. M. Townsley, D. A. Chamulak, E. F. Brown, and F. X. Timmes. 2010. Evaluating systematic dependencies of type Ia supernovae: The influence of deflagration to detonation density. *ApJ* 720: 99–113.
- Jordan IV, G. C., R. T. Fisher, D. M. Townsley, A. C. Calder, C. Graziani, S. Asida, D. Q. Lamb, and J. W. Truran. 2008. Three-dimensional simulations of the deflagration phase of the gravitationally confined detonation model of Type Ia supernovae. *ApJ* 681: 1448–1457.
- Jordan IV, G. C., C. Graziani, R. T. Fisher, D. M. Townsley, C. Meakin, K. Weide, L. B. Reid, J. Norris, R. Hudson, and D. Q. Lamb. 2012a. The detonation mechanism of the pulsationally assisted gravitationally confined detonation model of type Ia supernovae. *ApJ* 759: 53.
- Jordan IV, G. C., H. B. Perets, R. T. Fisher, and D. R. van Rossum. 2012b. Failed-detonation Supernovae: Subluminous Low-velocity Ia Supernovae and their Kicked Remnant White Dwarfs with Iron-rich Cores. *ApJ Lett.* 761: 23.
- Kasen, D., F. K. Röpke, and S. E. Woosley. 2009. The diversity of type Ia supernovae from broken symmetries. *Nature* 460: 869–872.
- Khokhlov, A. M. 1989. The structure of detonation waves in supernovae. *Mon. Not. R. Astron. Soc.* 239: 785–808.
- Khokhlov, A. M. 1991. Delayed detonation model for type Ia supernovae. *A&A* 245: 114–128.
- Khokhlov, A. M. 1995. Propagation of turbulent flames in supernovae. *ApJ* 449: 695–713.
- Kromer, M., M. Fink, V. Stanishev, S. Taubenberger, F. Ciaraldi-Schoolman, R. Pakmor, F. K. Röpke, A. J. Ruiter, I. R. Seitenzahl, S. A. Sim, G. Blanc, N. Elias-Rosa, and W. Hillebrandt. 2013. 3D deflagration simulations leaving bound remnants: a model for 2002cx-like Type Ia supernovae. *Mon. Not. R. Astron. Soc.* 429: 2287–2297.
- Landau, L. D., and E. M. Lifshitz. 1987. *Fluid mechanics (course of theoretical physics: volume 6)*, 2nd edn. Oxford: Butterworth-Heinemann.
- Lee, J. H. S., R. Knystautas, and N. Yoshikawa. 1978. Photochemical initiation of gaseous detonations. *Acta Astronautica* 5: 971–982.
- Liñan, Amable, and Forman A. Williams. 1993. *Fundamental aspects of combustion*. Oxford, New York: Oxford University Press.
- Lisewski, A. M., W. Hillebrandt, and S. E. Woosley. 2000. Constraints on the delayed transition to detonation in Type Ia supernovae. *ApJ* 538: 831–836.

- Maier, A., and J. C. Niemeyer. 2006. C+O detonations in thermonuclear supernovae: interaction with previously burned material. *A&A* 451: 207–212.
- Marquardt, K. S., S. A. Sim, A. J. Ruiter, I. R. Seitenzahl, S. T. Ohlmann, M. Kromer, R. Pakmor, and F. K. Röpke. 2015. Type Ia supernovae from exploding oxygen-neon white dwarfs. *A&A* 580: 118.
- Meakin, C. A., I. Seitenzahl, D. Townsley, G. C. Jordan, J. Truran, and D. Lamb. 2009. Study of the detonation phase in the gravitationally confined detonation model of Type Ia supernovae. *ApJ* 693: 1188–1208.
- Moll, R., and S. E. Woosley. 2013. Multi-dimensional Models for Double Detonation in Sub-Chandrasekhar Mass White Dwarfs. *ApJ* 774: 137.
- Niemeyer, J. C., and W. Hillebrandt. 1995. Turbulent nuclear flames in type Ia supernovae. *ApJ* 452: 769–778.
- Niemeyer, J. C., and W. Hillebrandt. 1997. Microscopic and macroscopic modeling of thermonuclear burning fronts. In *NATO ASIC Proc. 486: Thermonuclear supernovae*, eds. P. Ruiz-Lapuente, R. Canal, and J. Isern. Vol. 486 of *Nato asic proc.*, 441–456. Dordrecht: Kluwer Academic Publishers.
- Ohlmann, S. T., M. Kromer, M. Fink, R. Pakmor, I. R. Seitenzahl, S. A. Sim, and F. K. Röpke. 2014. The white dwarf’s carbon fraction as a secondary parameter of Type Ia supernovae. *A&A* 572: 57.
- Osher, S., and J. A. Sethian. 1988. Fronts propagating with curvature-dependent speed: Algorithms based on Hamilton–Jacobi formulations. *Journal of Computational Physics* 79: 12–49.
- Pakmor, R., M. Kromer, F. K. Röpke, S. A. Sim, A. J. Ruiter, and W. Hillebrandt. 2010. Sub-luminous type Ia supernovae from the mergers of equal-mass white dwarfs with mass  $\sim 0.9m_{\odot}$ . *Nature* 463: 61–64.
- Pakmor, R., M. Kromer, S. Taubenberger, S. A. Sim, F. K. Röpke, and W. Hillebrandt. 2012. Normal Type Ia supernovae from violent mergers of white dwarf binaries. *ApJ Lett.* 747: 10.
- Pakmor, R., M. Kromer, S. Taubenberger, and V. Springel. 2013. Helium-ignited violent mergers as a unified model for normal and rapidly declining type Ia supernovae. *ApJ Lett.* 770: 8.
- Peters, Norbert. 2000. *Turbulent combustion*. Cambridge: Cambridge University Press.
- Poludnenko, A. Y., T. A. Gardiner, and E. S. Oran. 2011. Spontaneous Transition of Turbulent Flames to Detonations in Unconfined Media. *Physical Review Letters* 107 (5): 054501.
- Reinecke, M., W. Hillebrandt, and J. C. Niemeyer. 2002a. Refined numerical models for multidimensional type Ia supernova simulations. *A&A* 386: 936–943.
- Reinecke, M., W. Hillebrandt, and J. C. Niemeyer. 2002b. Three-dimensional simulations of type Ia supernovae. *A&A* 391: 1167–1172.
- Reinecke, M., W. Hillebrandt, J. C. Niemeyer, R. Klein, and A. Gröbl. 1999. A new model for deflagration fronts in reactive fluids. *A&A* 347: 724–733.
- Röpke, F. K. 2003. On the stability of thermonuclear flames in type Ia supernova explosions. PhD diss, Technical University of Munich.
- Röpke, F. K. 2005. Following multi-dimensional type Ia supernova explosion models to homologous expansion. *A&A* 432: 969–983.
- Röpke, F. K. 2007. Flame-driven deflagration-to-detonation transitions in Type Ia supernovae? *ApJ* 668: 1103–1108.
- Röpke, F. K., and W. Hillebrandt. 2004. The case against the progenitor’s carbon-to-oxygen ratio as a source of peak luminosity variations in type Ia supernovae. *A&A* 420: 1–4.
- Röpke, F. K., and W. Hillebrandt. 2005. Full-star type Ia supernova explosion models. *A&A* 431: 635–645.
- Röpke, F. K., and J. C. Niemeyer. 2007. Delayed detonations in full-star models of type Ia supernova explosions. *A&A* 464: 683–686.
- Röpke, F. K., W. Hillebrandt, and J. C. Niemeyer. 2004a. The cellular burning regime in type Ia supernova explosions. I. Flame propagation into quiescent fuel. *A&A* 420: 411–422.
- Röpke, F. K., W. Hillebrandt, and J. C. Niemeyer. 2004b. The cellular burning regime in type Ia supernova explosions. II. Flame propagation into vortical fuel. *A&A* 421: 783–795.



- Röpke, F. K., J. C. Niemeyer, and W. Hillebrandt. 2003. On the small-scale stability of thermonuclear flames in Type Ia supernovae. *ApJ* 588: 952–961.
- Röpke, F. K., S. E. Woosley, and W. Hillebrandt. 2007b. Off-center ignition in Type Ia supernovae. I. initial evolution and implications for delayed detonation. *ApJ* 660: 1344–1356.
- Röpke, F. K., W. Hillebrandt, J. C. Niemeyer, and S. E. Woosley. 2006. Multi-spot ignition in type Ia supernova models. *A&A* 448: 1–14.
- Röpke, F. K., W. Hillebrandt, W. Schmidt, J. C. Niemeyer, S. I. Blinnikov, and P. A. Mazzali. 2007a. A three-dimensional deflagration model for Type Ia supernovae compared with observations. *ApJ* 668: 1132–1139.
- Schmidt, W., J. C. Niemeyer, and W. Hillebrandt. 2006a. A localised subgrid scale model for fluid dynamical simulations in astrophysics. I. Theory and numerical tests. *A&A* 450: 265–281.
- Schmidt, W., J. C. Niemeyer, W. Hillebrandt, and F. K. Röpke. 2006b. A localised subgrid scale model for fluid dynamical simulations in astrophysics. II. Application to type Ia supernovae. *A&A* 450: 283–294.
- Seitenzahl, I. R., F. Ciaraldi-Schoolmann, F. K. Röpke, M. Fink, W. Hillebrandt, M. Kromer, R. Pakmor, A. J. Ruiter, S. A. Sim, and S. Taubenberger. 2013. Three-dimensional delayed-detonation models with nucleosynthesis for Type Ia supernovae. *Mon. Not. R. Astron. Soc.* 429: 1156–1172.
- Seitenzahl, I. R., M. Kromer, S. T. Ohlmann, F. Ciaraldi-Schoolmann, K. Marquardt, M. Fink, W. Hillebrandt, R. Pakmor, F. K. Röpke, A. J. Ruiter, S. A. Sim, and S. Taubenberger. 2016. Three-dimensional simulations of gravitationally confined detonations compared to observations of SN 1991T. *A&A* 592: 57.
- Sharpe, G. J. 1999. The structure of steady detonation waves in Type Ia supernovae: pathological detonations in C-O cores. *Mon. Not. R. Astron. Soc.* 310: 1039–1052.
- Sim, S. A., F. K. Röpke, W. Hillebrandt, M. Kromer, R. Pakmor, M. Fink, A. J. Ruiter, and I. R. Seitenzahl. 2010. Detonations in sub-Chandrasekhar-mass C+O white dwarfs. *ApJ Lett.* 714: 52–57.
- Timmes, F. X., and S. E. Woosley. 1992. The conductive propagation of nuclear flames. I. degenerate C+O and O+Ne+Mg white dwarfs. *ApJ* 396: 649–667.
- Timmes, F. X., M. Zingale, K. Olson, B. Fryxell, P. Ricker, A. C. Calder, L. J. Dursi, H. Tufo, P. MacNeice, J. W. Truran, and R. Rosner. 2000. On the Cellular Structure of Carbon Detonations. *ApJ* 543: 938–954.
- Toro, E. F. 2009. *Riemann solvers and numerical methods for fluid dynamics: A practical introduction*. Berlin Heidelberg: Springer. <http://books.google.de/books?id=SqEjX0um8o0C>.
- Townsend, D. M., A. C. Calder, S. M. Asida, I. R. Seitenzahl, F. Peng, N. Vladimirova, D. Q. Lamb, and J. W. Truran. 2007. Flame evolution during Type Ia supernovae and the deflagration phase in the gravitationally confined detonation scenario. *ApJ* 668: 1118–1131.
- Townsend, D. M., A. P. Jackson, A. C. Calder, D. A. Chamulak, E. F. Brown, and F. X. Timmes. 2009. Evaluating systematic dependencies of Type Ia supernovae: The influence of progenitor  $^{22}\text{Ne}$  content on dynamics. *ApJ* 701: 1582–1604.
- Vladimirova, N., G. V. Weirs, and L. Ryzhik. 2006. Flame capturing with an advection-reaction-diffusion model. *Combustion Theory Modelling* 10 (5): 727–747.
- von Neumann, J. 1942. Theory of detonation waves, Prog. Rept. No. 238; O.S.R.D. Rept. No. 549, Ballistic Research Laboratory File No. X-122, Aberdeen Proving Ground, MD, Aberdeen Proving Ground, MD.
- Woosley, S. E., A. R. Kerstein, V. Sankaran, A. J. Aspdén, and F. K. Röpke. 2009. Type Ia Supernovae: Calculations of Turbulent Flames Using the Linear Eddy Model. *ApJ* 704: 255–273.
- Zel’dovich, Y. B. 1940. On the theory of the propagation of detonations on gaseous system. *Zh. Eksp. Teor. Fiz.* 10: 542–568. In Russian..
- Zel’dovich, Y. B. 1966. An effect which stabilizes the curved front of a laminar flame. *Journal of Applied Mechanics and Technical Physics* 7: 68–69.
- Zel’dovich, Y. B., V. B. Librovich, G. M. Makhviladze, and G. I. Sivashinskii. 1970. On the onset of detonation in a nonuniformly heated gas. *Journal of Applied Mechanics and Technical Physics* 11: 264–270.